



Half-sandwich arene ruthenium, rhodium and iridium thiosemicarbazone complexes: synthesis, characterization and biological evaluation

AGREEDA LAPASAM^a, VENKANNA BANOTHU^b, UMA ADDEPALLY^b and MOHAN RAO KOLLIPARA^{a,*} 

^aCentre for Advanced Studies in Chemistry, North-Eastern Hill University, Shillong 793 022, Meghalaya, India

^bCentre for Biotechnology (CBT), Institute of Science & Technology (IST), Jawaharlal Nehru Technological University Hyderabad (JNTUH), Kukatpally, Hyderabad, Telangana 500 085, India
E-mail: mohanrao59@gmail.com; kmrao@nehu.ac.in

MS received 30 August 2019; revised 4 October 2019; accepted 9 October 2019

Abstract. A series of ruthenium, rhodium and iridium complexes with 4-phenyl-1-(pyridin-4yl)methylene thiosemicarbazide (L1) and 4-phenyl-1-(pyridin-4yl)ethylidene thiosemicarbazide (L2) ligands were synthesized and isolated with hexafluorophosphate as a counter ion. All these complexes were fully characterized with the help of FT-IR, UV-Vis, ¹H NMR, ¹³C NMR and elemental analysis. An agar-well diffusion method was employed for evaluation of antibacterial activities against one Gram-positive bacteria *Staphylococcus aureus* and two Gram-negative bacteria *Escherichia coli*, *Klebsiella pneumoniae*. Antimicrobial activity evaluation revealed that Cp* rhodium complexes has a significant antibacterial activity for all the three strains, Cp* iridium and *p*-cymene ruthenium complexes have shown moderated activity against the microorganisms but none of the complexes surpass the activity of their reference drugs. Results indicated that all the complexes reported here inhibit the growth of bacteria.

Keywords. Ruthenium; rhodium; iridium; thiosemicarbazide; antibacterial.

1. Introduction

For many years, new drugs of an interesting structure, unknown molecular target, low toxicity and a high therapeutic index have been looked for. This is due to the impossibility of treating many serious diseases, such as bacterial infections or cancer. The ruthenium arene-based drugs have attracted particular interest in recent years.^{1,2} Beside platinum compounds, piano-stool ruthenium half-sandwich complexes are the very promising class of antimicrobial and antitumor agents as the stereochemistry of these complexes offers a good platform for producing new molecules by changing the chelated ligand, coordinated arene and the labile group.^{3,4} In addition, both the commonly accessible oxidation states of ruthenium (II and III) are octahedral and relatively inert.⁵ Cp*Rh and Cp*Ir complexes have also been considered as alternatives to

ruthenium-based drugs mainly because of their water solubility which allows half-sandwich complexes to be easily tailored for catalytic or biological applications. The interesting chemical properties exhibited by the complexes of rhodium metal encourage the large considerable current attention of rhodium chemistry.^{6,7} The anticancer activity of iridium complexes have made great progress, where a number of iridium complexes show high anticancer effect.^{8–10} But there are relatively few reports on the antimicrobial properties of organometallic iridium complexes.^{11,12} The results available to date strongly indicate that organometallic compounds have greatly contributed to the interest in synthesizing new metals complexes and investigating their biological applications.

Last few years, pronounced number of Schiff base complexes of transition metal prompted wide interest because of their wide range of pharmacological effects.

*For correspondence

Electronic supplementary material: The online version of this article (<https://doi.org/10.1007/s12039-019-1731-5>) contains supplementary material, which is available to authorized users.

Thiosemicarbazones (TSCs) are Schiff-base type compounds that have three potential donor sites (N1, N2 atoms and one S atom), which endow them multiple coordination modes when coordinate to metals leading to the formation of either a five or a four-member chelate ring,^{13–16} generally, act as bidentate chelating for various metal ions by bonding through the sulfur atom and the hydrazinic nitrogen atom. Thiosemicarbazones and their metal complexes have attracted considerable attention by chemists and biologists because it displayed a wide spectrum of biological activities,^{17–19} in particular, they possess antiparasitic, antibacterial, anticancer, and antiviral properties.^{20–30} Also, the metal thiosemicarbazone complexes exhibit higher biological activities than the thiosemicarbazone ligand itself. Ruthenium arene complexes having thiosemicarbazones have been evolving as promising parasitic and therapeutic agents.^{31–36}

Recently we have reported the synthesis and antibacterial activities of ruthenium, rhodium and iridium metal complexes containing various Schiff-base ligands.^{37,38} In continuation of our previous work, the target of the current work was to report the synthesis of thiosemicarbazide ligands, their metals complexes and evaluation of all the compounds as the possible antibacterial agents (Chart 1).

2. Experimental Methods

2.1 Physical methods and materials

All reagents used in this work were purchased commercially and used without further purification; 4-acetyl pyridine, 4-pyridine carbaldehyde and 4-phenyl thiosemicarbazide were purchased from Alfa Aesar. Metal chloride's $\text{RuCl}_3 \cdot n\text{H}_2\text{O}$, $\text{RhCl}_3 \cdot n\text{H}_2\text{O}$ and $\text{IrCl}_3 \cdot n\text{H}_2\text{O}$ were purchased from Arora Matthey Limited. Pentamethylcyclopentadiene and α -Terpinene were obtained from Sigma Aldrich. Starting compounds $[\text{Cp}^*\text{MCl}_2]_2$ ($\text{M} = \text{Rh}/\text{Ir}$) were synthesized using an Anton Paar monowave 50 synthesizer in 10 mL microwave vials equipped with magnetic stirring bars as previously reported.³⁹ The syntheses of all the metal complexes were

performed at room temperature. Infrared (IR) spectra were recorded on a Bruker ALPHA II FTIR spectrometer as KBr pellets in the range 4000 to 400 cm^{-1} . ^1H NMR spectra were recorded on a Bruker Avance II 400 MHz spectrometer using CDCl_3 and DMSO-d_6 as solvents, with TMS as internal references at room temperature. UV–Vis absorption spectra were obtained on a Perkin-Elmer Lambda 25 UV/Vis spectrophotometer in acetonitrile solution at room temperature. Conductance measurements were carried out in acetonitrile solutions using a Wayne Kerr model 6440A Component Analyzer and a dip-type conductivity cell with platinized platinum electrodes. Mass Spectra were recorded using Agilent 6540 UHD Accurate-Mass Q-TOF LC/MS instrument. Elemental analyses of the complexes were carried out on a Perkin-Elmer 2400 CHN analyzer.

2.2 Antimicrobial activity

All the Gram-negative and Gram-positive bacterial strains used for the present study were obtained from the Department of Microbiology, Osmania General Hospital, Hyderabad. All strains were tested for purity by standard microbiological methods. The bacterial stock cultures were maintained on Mueller-Hinton agar slants and stored at 4 °C. An agar-well diffusion method was employed for the evaluation of antibacterial activities of test compounds.^{40,41} DMSO was used as a negative control. The bacterial strains were reactivated from stock cultures by transferring into Mueller-Hinton broth and incubating at 37 °C for 18 h. A final inoculum containing 10^6 colonies forming units (1×10^6 CFU/mL) was added aseptically to MHA medium and poured into sterile petri dishes. Different test compounds at a concentration of 100 μg per well were added to wells (8 mm in diameter) punched on agar surface. Plates were incubated overnight at 37 °C and diameter of inhibition zone (DIZ) around each well was measured in mm. Experiments were performed in triplicates (Error bars with percentage and standard deviation).

2.3 MIC & MBC

The minimum inhibitory concentration (MIC) and minimum bactericidal concentration (MBC) was determined by the

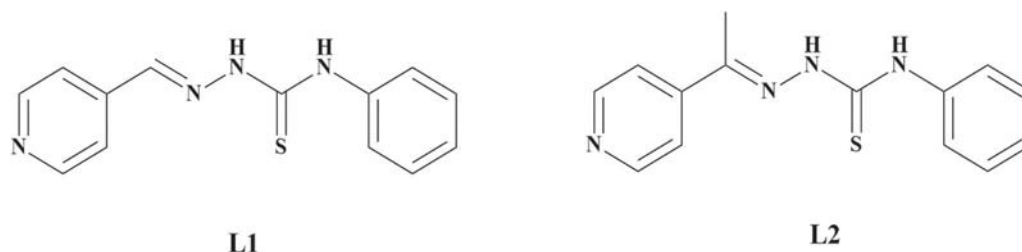


Chart 1. Ligand used in the present study.

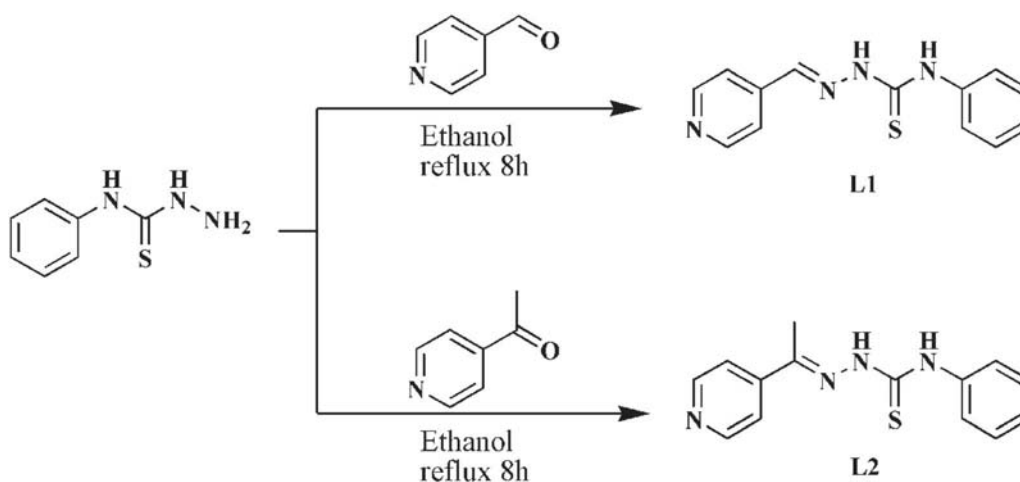
micro-broth dilution method done in 96 well plates according to standard protocol.⁴² A 2-fold serial dilution of the compounds, with the appropriate antibiotic, was prepared. Initially, 100 μL of MH broth was added to each well plate. Then 100 μL of compound or antibiotic was taken from the stock solution and dissolved in the first well plate. Serial dilution was done to obtain different concentrations. The stock concentrations of 2.0 mg/mL. 24 h culture turbidity was adjusted to match 0.5 McFarland standards which correspond to 1×10^8 CFU/ml. The standardized suspension (100 μL) of bacteria was added to all the wells except the antibiotic control well and the 96 well plates were incubated at 37 $^\circ\text{C}$ for 24 h. After 24 h of incubation 40 μL of MTT (3-(4,5-dimethylthiazol-2-yl)-2,5-diphenyltrazolium bromide) reagent (0.1 mg/mL in 1x PBS) was added to all the wells. MIC was taken as the lowest concentration which did not show any growth which was visually noted from the blue color developed by MTT. Subcultures were made from clear wells and the lowest concentration that yielded no growth after subculturing was taken as the MBC.

2.4 Synthesis of ligands

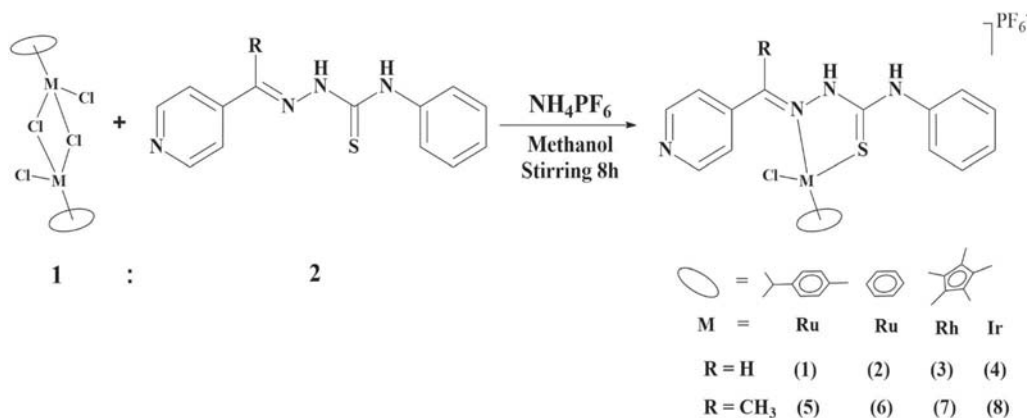
The ligands 4-phenyl-1-(pyridin-4yl)methylene thiosemicarbazide (L1), 4-phenyl-1-(pyridin-4yl)ethylidene thiosemicarbazide (L2), were made by the condensation of phenyl thiosemicarbazide with appropriate pyridine (Scheme 1).⁴³ The solution was evaporated under reduced pressure, an orange and yellow solid was obtained and it was washed with diethyl ether and dried in vacuum.

2.5 Synthesis of complexes (1–8)

A mixture of starting metal precursor (0.1 mmol), ligands (0.2 mmol) and (1 mmol) of NH_4PF_6 were dissolved in dry methanol (10 mL) and stirred at room temperature for 8 h (Scheme 2). A yellow colored compound precipitated out from the reaction mixture. The precipitate was filtered, washed with cold methanol and diethyl ether and dried.



Scheme 1. Synthesis of ligands.



Scheme 2. Synthesis of complexes 1–8.

2.5a [(*p*-cymene)RuL1Cl]PF₆ [1]: Yield: 82%; IR (KBr, cm⁻¹): 3446ν_(N-H), 1616ν_(C=N), 844 ν_(P-F), 757_(C=S); ¹H NMR (400 MHz, CDCl₃, ppm): 11.28 (s, 1H), 10.00 (s, 1H), 8.61 (s, 1H), 8.01 (d, 1H, *J* = 8Hz), 7.91 (d, 1H, *J* = 8Hz), 7.72 (d, 1H, *J* = 8Hz), 7.53 (t, 1H, *J* = 8Hz), 7.44 (d, 2H, *J* = 8Hz), 7.39 (d, 1H, *J* = 8Hz), 7.12 (d, 1H, *J* = 8Hz), 6.98 (t, 1H, *J* = 8Hz), 5.49 (d, 2H, *J* = 8Hz), 5.35 (d, 2H, *J* = 4Hz), 2.93 (sept, 1H), 2.17 (s, 3H), 1.29 (d, 6H, *J* = 8Hz); ¹³C NMR (100 MHz, CDCl₃, ppm): 180.70, 156.08, 149.62, 139.84, 136.54, 132.36, 129.96, 127.83, 123.23, 100.95, 98.72, 88.29, 88.07, 86.12, 85.46, 34.03, 25.90, 21.38; UV-Vis {Acetonitrile, λ_{max}, nm (ε/10⁻⁴ M⁻¹ cm⁻¹): 269.97 (3.128), 375.07 (1.97), 440.06 (1.59); ESI-MS (m/z): 527.062 [M-PF₆]⁺; Anal. Calc. for C₂₃H₂₆ClN₄SRuPF₆ (672.03): C, 41.11; H, 3.90; N, 8.34. Found: C, 41.24; H, 3.88; N, 8.41%.

2.5b [(benzene)RuL1Cl]PF₆ [2]: Yield: 74%; IR (KBr, cm⁻¹): 3449ν_(N-H), 1617ν_(C=N), 845ν_(P-F), 757_(C=S); ¹H NMR (400 MHz, DMSO-d₆, ppm): 11.19 (s, 1H), 9.92 (s, 1H), 9.71(s, 1H), 8.06 (d, 2H, *J* = 8Hz), 7.66 (d, 3H, *J* = 8Hz), 7.38 (t, 1H, *J* = 8Hz), 6.93 (d, 1H, *J* = 8Hz), 6.72 (d, 1H, *J* = 8Hz) 6.56 (t, 1H, *J* = 8Hz), 5.92 (s, 6H); UV-Vis {Acetonitrile, λ_{max}, nm (ε/10⁻⁴ M⁻¹ cm⁻¹): 269.97 (4.301), 369.95 (2.404), 544.96 (0.859); Anal. Calc. for C₁₉H₁₈ClN₄SRuPF₆ (615.93): C, 37.05; H, 2.95; N, 9.10. Found: C, 37.16; H, 3.01; N, 9.07%.

2.5c [Cp*RhL1Cl]PF₆ [3]: Yield: 79%; IR (KBr, cm⁻¹): 3450ν_(N-H), 1667ν_(C=N), 847ν_(P-F), 756_(C=S); ¹H NMR (400 MHz, CDCl₃, ppm): 11.07 (s, 1H), 10.50 (s, 1H), 9.82 (s, 1H), 8.06 (d, 1H, *J* = 8Hz), 7.86 (d, 2H, *J* = 8Hz), 7.35 (t, 3H, *J* = 4Hz), 6.88 (s, 2H), 6.69 (s, 1H), 1.65 (s, 15H); ¹³C NMR (100 MHz, CDCl₃, ppm): 179.21, 152.64, 150.38, 137.87, 134.09, 131.36, 128.83, 125.87, 123.77, 120.02, 91.33, 8.36; UV-Vis {Acetonitrile, λ_{max}, nm (ε/10⁻⁴ M⁻¹ cm⁻¹): 229.07 (6.992), 269.67 (7.413), 365.04 (5.562), 559.01 (1.268); ESI-MS (m/z): 529.205 [M-PF₆]⁺; Anal. Calc. for C₂₃H₂₇ClN₄SRhPF₆ (674.87): C, 40.93; H, 4.03; N, 8.30. Found: C, 40.91; H, 4.06; N, 8.38%.

2.5d [Cp*IrL1Cl]PF₆ [4]: Yield: 67%; IR (KBr, cm⁻¹): 3448ν_(N-H), 1633ν_(C=N), 849ν_(P-F), 686_(C=S); ¹H NMR (400 MHz, CDCl₃, ppm): 11.23 (s, 1H), 10.04 (s, 1H), 9.95 (s, 1H), 7.98 (d, 2H, *J* = 8Hz), 7.83 (d, 1H, *J* = 8Hz), 7.41 (d, 1H, *J* = 8Hz), 7.30 (t, 2H, *J* = 4Hz), 6.96 (d, 2H, *J* = 4Hz), 6.81 (s, 1H), 1.60 (s, 15H); UV-Vis {Acetonitrile, λ_{max}, nm (ε/10⁻⁴ M⁻¹ cm⁻¹): 269.97 (6.037), 355.00 (3.506), 510 (1.0183); Anal. Calc. for C₂₃H₂₇ClN₄SIrPF₆ (764.19): C, 36.15; H, 3.56; N, 7.33. Found: C, 36.27; H, 3.63; N, 7.47%.

2.5e [(*p*-cymene)RuL2Cl]PF₆ [5]: Yield: 83%; IR (KBr, cm⁻¹): 3449ν_(N-H), 1601ν_(C=N), 845ν_(P-F), 756_(C=S); ¹H NMR (400 MHz, CDCl₃, ppm): 11.35 (s, 1H), 10.49 (s, 1H), 9.84 (d, 1H, *J* = 16Hz), 8.07 (d, 1H, *J* = 4Hz), 7.87 (d, 2H, *J* = 8Hz), 7.34 (d, 2H, *J* = 8Hz), 6.87 (s, 2H), 6.67 (s,

1H), 5.49 (d, 2H, *J* = 4Hz), 5.36 (d, 2H, *J* = 8Hz), 2.91 (sept, 1H), 2.42 (s, 3H), 2.15 (s, 3H), 1.28 (d, 6H, *J* = 8Hz); UV-Vis {Acetonitrile, λ_{max}, nm (ε/10⁻⁴ M⁻¹ cm⁻¹): 274.02 (5.809), 369.22 (2.684), 475.26 (1.536); Anal. Calc. for C₂₄H₂₈ClN₄SRuPF₆ (686.06): C, 42.02; H, 4.11; N, 8.17. Found: C, 41.99; H, 4.16; N, 8.19%.

2.5f [(benzene)RuL2Cl]PF₆ [6]: Yield: 71%; IR (KBr, cm⁻¹): 3449ν_(N-H), 1634ν_(C=N), 845ν_(P-F), 755_(C=S); ¹H NMR (400 MHz, CDCl₃, ppm): 11.36 (s, 1H), 9.73 (s, 1H), 7.98 (d, 2H, *J* = 12Hz), 7.69 (d, 2H, *J* = 8Hz), 7.29 (d, 2H, *J* = 8Hz), 6.81 (d, 1H, *J* = 4Hz), 6.70 (t, 2H, *J* = 8Hz), 5.90 (s, 6H), 2.33(s, 3H); ¹³C NMR (100 MHz, DMSO-d₆, ppm): 178.40, 152.35, 140.78, 136.33, 131.27, 127.49, 127.27, 120.53, 87.83, 17.15; UV-Vis {Acetonitrile, λ_{max}, nm (ε/10⁻⁴ M⁻¹ cm⁻¹): 275.41 (3.3858), 370.07 (2.496), 450.02 (2.041); ESI-MS (m/z): 485.117 [M-PF₆]⁺; Anal. Calc. for C₂₀H₂₀ClN₄SRuPF₆ (629.95): C, 38.13; H, 3.20; N, 8.89. Found: C, 38.23; H, 3.22; N, 8.97%.

2.5g [Cp*RhL2Cl]PF₆ [7]: Yield: 84%; IR (KBr, cm⁻¹): 3448ν_(N-H), 1599ν_(C=N), 846ν_(P-F), 766_(C=S); ¹H NMR (400 MHz, CDCl₃, ppm): 11.20 (s, 1H), 9.78 (s, 1H), 8.90 (d, 1H, *J* = 8 Hz), 7.97 (d, 1H, *J* = 8 Hz), 7.90 (s, 1H) 7.81 (t, 1H, *J* = 4Hz), 7.73 (t, 1H, *J* = 4Hz), 7.30 (d, 2H, *J* = 8Hz), 7.23 (d, 1H, *J* = 4Hz), 7.08 (d, 1H, *J* = 8Hz), 2.39 (s, 3H) 1.56 (s, 15H); ¹³C NMR (100 MHz, CDCl₃, ppm): 177.92, 157.99, 150.56, 141.51, 137.12, 133.73, 129.96, 125.93, 123.63, 96.06, 17.11, 10.93; UV-Vis {Acetonitrile, λ_{max}, nm (ε/10⁻⁴ M⁻¹ cm⁻¹): 274.97 (7.841), 350.02 (3.7783), 470.06 (1.180); Anal. Calc. for C₂₄H₂₉ClN₄SRhPF₆ (688.90): C, 41.84; H, 4.24; N, 8.13. Found: C, 41.95; H, 4.32; N, 8.20%.

2.5h [Cp*IrL2Cl]PF₆ [8]: Yield: 73%; IR (KBr, cm⁻¹): 3448ν_(N-H), 1621ν_(C=N), 846ν_(P-F), 757_(C=S); ¹H NMR (400 MHz, CDCl₃, ppm): 11.28 (s, 1H), 10.50 (s, 1H), 8.72 (d, 1H, *J* = 20Hz), 7.91 (d, 1H, *J* = 8Hz), 7.67 (d, 2H, *J* = 8Hz), 7.24 (d, 2H, *J* = 8Hz), 6.68 (t, 3H, *J* = 4Hz), 2.31(s, 3H), 1.62 (s, 15H); ¹³C NMR (100 MHz, DMSO-d₆, ppm): 175.42, 156.17, 146.88, 137.30, 131.92, 129.28, 128.94, 128.74, 128.42, 127.16, 125.22, 121.58, 93.07, 7.88; UV-Vis {Acetonitrile, λ_{max}, nm (ε/10⁻⁴ M⁻¹ cm⁻¹): 270.00 (6.428), 364.52 (5.248), 505.00 (1.083); ESI-MS (m/z): 633.124 [M-PF₆]⁺; Anal. Calc. for C₂₄H₂₉ClN₄SIrPF₆ (778.21): C, 37.04; H, 3.76; N, 7.20. Found: C, 37.21; H, 3.82; N, 7.31%.

3. Results and Discussion

3.1 Synthesis of complexes

Thiosemicarbazide ligands were allowed to react with the metal precursor [Ru(*p*-cymene)Cl₂]₂, [Cp*RhCl₂]₂ or [Cp*IrCl₂]₂ in a 1:2 M ratio in methanol in the presence of NH₄PF₆. The new complexes 1–8 of the

general formula, [(arene)M($\kappa^2_{(N,S)}L$)Cl]PF₆ were isolated as cationic complexes with their hexafluorophosphate salts as counter ion as presented in Scheme 2. All these metal complexes were obtained in good yield, air-stable and non-hygroscopic in nature. The complexes are soluble in polar solvents such as acetone, acetonitrile, DMSO and DMF, but are insoluble in non-polar solvents such as hexane and diethyl ether. The synthesized complexes were characterized by various spectroscopic techniques like ¹H-NMR, ¹³C-NMR, IR, UV-Vis and elemental analysis.

3.2 Spectral studies of complexes

The preliminary validation of the complex formation can be confirmed to some extent from their IR spectra (Figure S1–S8, Supplementary Information). The FT-IR spectra of the ligands show bands around 3400 cm⁻¹, assigning the highest absorptions corresponding to the N-H stretching frequency. Spectra of the complexes showed bands in the range 3446–3450 cm⁻¹, which were assigned to the two N–H bonds $\nu_{(sym)}$ stretching frequencies, and it has been found that there is no shift in their stretching frequencies upon complexation which mean that the N-H group did not form any bond with the metal ion. The azomethine (C=N) stretching frequencies of the free ligands were observed at 1639–1667 cm⁻¹ and a sharp band was observed at 816 and 812 cm⁻¹, ascribed to (C=S) stretching frequency of the ligands. The azomethine (C=N) and the thiocarbonyl C=S stretching frequency of the complexes was found in the range 1599–1637 cm⁻¹ and 755–766 cm⁻¹. All the values are in accordance with the previous reported.⁴⁴ The clear shift of the $\nu_{C=N}$ and $\nu_{C=S}$ vibration bands to a lower frequency value suggested that the thiosemicarbazone ligands coordinated to metal center through azomethine nitrogen and thiocarbonyl sulfur. In addition, all the complexes show distinctive stretching frequencies for P-F counter anions in the range of 844–849 cm⁻¹.

To ratify the formation and coordination pattern of metal complexes the ¹H NMR studies of the ligands and complexes were recorded in deuterated chloroform or dimethyl sulfoxide at room temperature (Figure S9–S16, Supplementary Information). The ¹H NMR spectra of the ligands, N-H protons appeared at 11.57 and 10.61 ppm, respectively, The ¹H NMR spectra of complexes 1–8 exhibit two singlet in the range 11.36–11.07 and 10.50–9.73 ppm corresponding to the two NH protons and its slightly shift upfield with respect to the free ligand indicating the co-ordination of the ligand to the metal center. The presence of two N-H signals in all the complexes specifies that

the N-H groups are not involved in bonding to the metals center.^{32,45} The azomethine proton of complexes 1–4 was observed as a singlet in the downfield region at 8.71, 9.61, 9.82 and 9.95 ppm, respectively indicating the co-ordination of the azomethine nitrogen to the metal center which arises due to the donation of lone pairs of the electron to the metal center. The ligand methyl proton signal for complexes 5–8 appeared as a singlet at 2.42, 2.33, 2.39, 2.31 ppm respectively. Resonances due to the aromatic ligands protons were all in the expected range of 9.84–6.56 ppm. Complexes 1 and 5 display a singlet and septet in the range 2.17–2.43 ppm and 2.93–2.91 ppm corresponding to the methyl group and methine protons of the isopropyl group of the p-cymene ligand. The signal for the methyl protons of the isopropyl group is observed as one doublet at 1.29 and 1.28 ppm for complexes 1 and 5. The resonance for the six protons of benzene in complexes 2 and 6 was observed at 5.92 and 5.90 ppm. In addition, a singlet at 1.65, 1.66, 1.56, 1.62 ppm is observed for complexes 3, 4, 7 and 8, respectively, corresponding to the methyl protons of the pentamethyl cyclopentadienyl ring.

The ¹³C NMR spectra of the complexes further explain the formation of complexes. The ¹³C NMR spectra of the representative complexes are provided in Figures S17–S21, Supplementary Information. The ¹³C NMR spectra of the complexes exhibited signals related with the ligand carbons, p-cymene ligand carbons, ring carbon of benzene, methyl carbon of Cp* and ring carbon of Cp*. The carbon resonance of the thiocarbonyl (C=S) group appeared in the lower frequency region around 175.42 to 180.70 ppm. The aromatic carbons signals for the ligands were observed in the range of 120.02 to 157.99 ppm. The methyl, isopropyl carbon and methine resonances of the p-cymene ligand were detected at 21.38, 25.90 and 34.03 ppm. Peaks at 100.95, 98.72, 88.29, 88.07 ppm assigned to the aromatic carbon of p-cymene ring. Complexes 6 exhibited a sharp peak at 87.83 ppm assigned to the carbon of benzene ring. The signals associated with the ring carbons of the Cp* ligand was observed in the region 91.33 to 96.06 ppm, whereas, the methyl carbon resonances were observed as a sharp peak in the range 7.88 to 10.93 ppm. Overall results from the NMR spectral studies intensely support the formation of the metal complexes.

The m/z values of the representative complexes are listed in the experimental section and are presented in the Figures S22–S25, Supplementary Information. Complexes 1, 3, 6 and 8 display their predominant peaks at m/z: 527.062, 529.205, 485.117, and 633.124 respectively correspond to [M-PF₆]⁺ ion peak. The

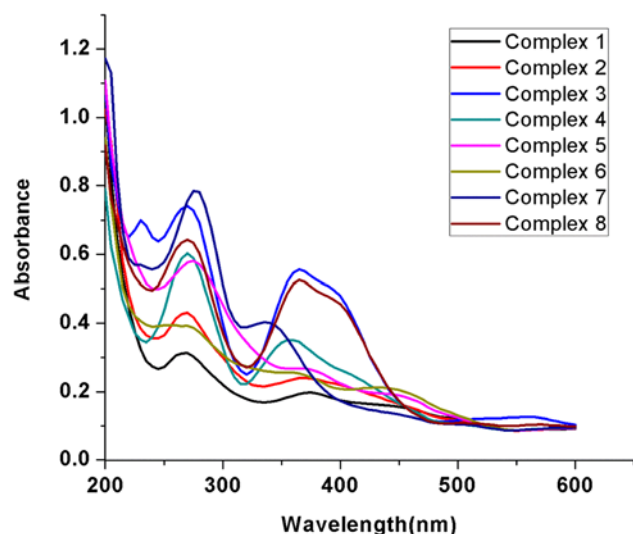


Figure 1. UV-Vis absorption spectra of complexes 1–8 at 10 μM acetonitrile solutions.

appearance of these peaks in its mass spectra strongly supports the formation of complexes.

The UV-visible spectra of complexes 1–8 were recorded in 10 μM acetonitrile solutions in the range 200–600 nm. All the complexes showed three bands around 270, 375 and 500 nm. The high intense band around 270 nm is attributed to $n \rightarrow \pi^*$, band at the lower wavelengths at 375 nm assigned to $\pi \rightarrow \pi^*$ transitions. Whereas, the lower energy absorption band in the region 500 nm are ascribed to metal to ligand charge transfer (MLCT) arises from the excitation of electrons from the metal t_{2g} level to the empty molecular orbitals π^* level of the ligands (Figure 1).

3.3 Conductivity measurement

The specific conductance values of complexes 1–8 of 0.001 molar concentration in acetonitrile solutions were recorded at room temperature are 221, 248, 253, 216, 170, 151, 337, 157 $\mu\text{S cm}^{-1}$ respectively. The value of ionic conductance is due to the presence of ionic moieties. These results reveal the electrolytic nature of metal complexes.

3.4 Stability studies

Due to the inadequate aqueous solubility of the metal complexes, antibacterial assay were carried out using stock solutions prepared by dissolution of the compound in Dimethyl Sulfoxide (DMSO). There is a possibility that chloride ligand of metal complexes could undergo a ligand exchange with the DMSO molecule and that would affect the value of

antibacterial determination, so the solution of all the complexes was investigated in DMSO. UV-Visible of the complexes 1–8 were recorded at room temperature in the range 200–600 nm. The electronic absorption spectra of the ligands and complexes were depicted in Figures S26 and S27, Supplementary Information. The analysis was performed by monitoring the solution at different time intervals up to 48 h to mimic the biological test conditions. No changes in the UV-Vis spectra were noticed, signifying that the complexes are stable in DMSO solution.

3.5 Antibacterial activity

Infections due to different pathogenic bacteria are a terrible danger to humankind. Dangerous strains of *E. coli* can cause urinary tract infections, gastroenteritis, and neonatal meningitis. *S. aureus* infection causes a severe disease staphylococcal scalded skin syndrome (SSSS) in infants and mastitis in cow. *K. pneumoniae* leads to the awful disease pneumonia. The antibacterial activity of the ligands and its metal complexes were evaluated against selected bacterial strains gram-positive bacteria *Staphylococcus aureus*, two gram-negative bacteria *Escherichia coli*, and *Klebsiella pneumoniae* by using standard techniques, ciprofloxacin was taking as a reference drug. Experiments for each condition were performed in triplicate. The starting precursor of [(arene)RuCl₂]₂, [Cp*RhCl₂]₂ and [Cp*IrCl₂]₂ were found to be inactive as reported in the previous literature.³⁷ Metal complexes often show better biological bacterial activities as compared to their ligands; therefore, the formation of complexes is generally accompanied by the improvement of antibacterial activity.⁴⁶ The potency of an antibacterial agent is based on the size of the diameter of zones of inhibition against the tested bacterial strain. The zones of inhibition (mm) of the compounds in comparison with ciprofloxacin were given in Table S1 (Supplementary Information) and graphically represented in Figure 2. Both the ligands L1 and L2 show significant activity against gram-positive bacteria *Staphylococcus aureus*. However, it did not show any noticeable activity against the gram-negative bacteria.

In-vitro assay results revealed that all the synthesized complexes (except complex 1) show potent antibacterial activity, among the complexes evaluated complex 5, Cp* rhodium complexes 3 and 7 shows a magnificent activity against all the tested bacterial strain. Complexes 3 and 7 showed highest activity against *Staphylococcus aureus* (15 ± 0.22 mm and 16 ± 0.78 mm), *Escherichia coli* (15 ± 0.02 mm and 16

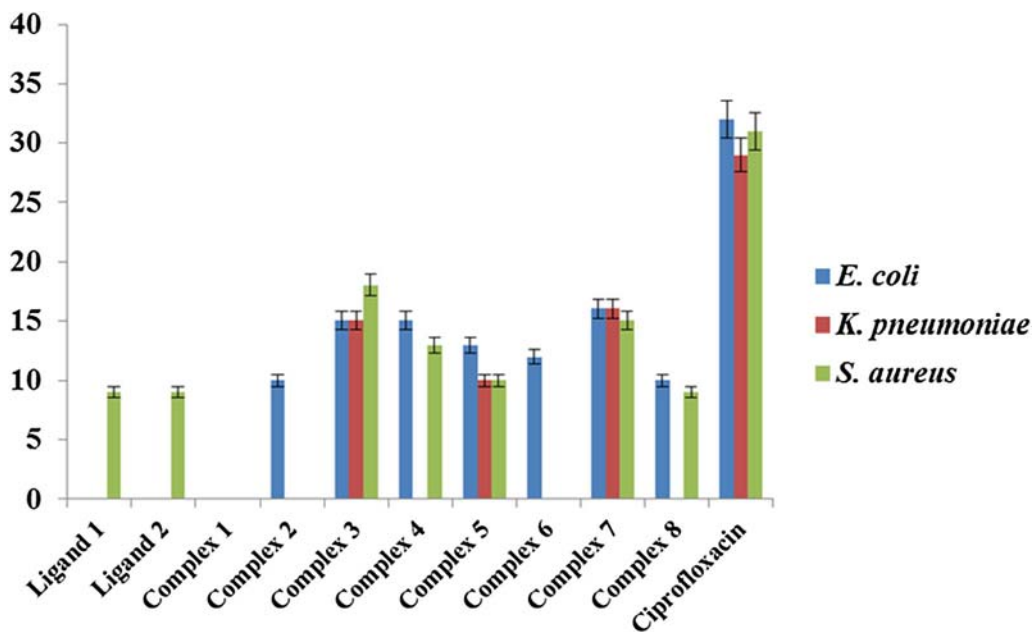


Figure 2. Histogram of the zone of inhibition in mm obtained by the ligands 1–2 and complexes 1–8 in comparison to the standard Ciprofloxacin. All the complexes expressed standard deviation of error within the ± 1 .

± 0.92 mm,) *Klebsiella pneumoniae* (18 ± 0.43 mm and 15 ± 0.62 mm). Cp* iridium complexes 4 and 8 show potent activity against *Escherichia coli* and *Staphylococcus aureus*. Complexes 2 and 6, which are the benzene ruthenium complexes, show moderate activity against *Escherichia coli* strain only. As proof from the inhibitory potency rhodium complexes shows good activity compare to Cp*Ir and p-cymene ruthenium complexes while benzene ruthenium complexes

show minimum activity. Results obtained clearly indicate that the formation of metal complexes enhanced biological activities.

3.6 MIC and MBC

The minimum inhibitory concentration (MIC) and minimum bactericidal concentration (MBC) results

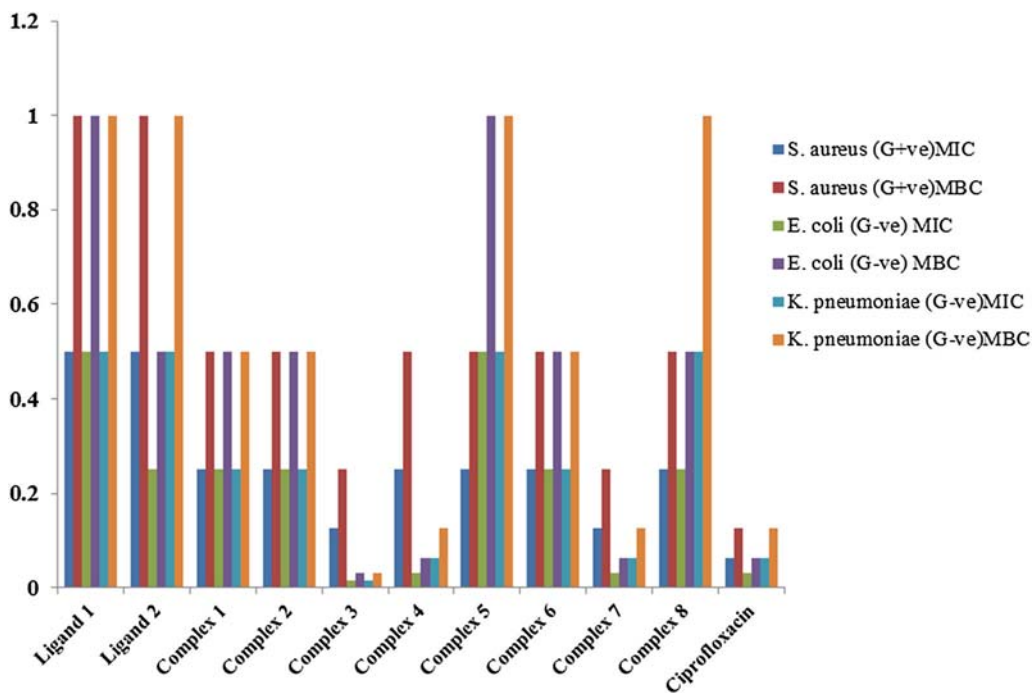


Figure 3. Selected antimicrobial data of ligands 1–2 and complexes 1–8 as minimum inhibitory concentration (MIC) and minimum bactericidal concentration (MBC) values in 2.0 mg/mL concentration.

were listed in Table S2 (Supplementary Information) and graphically represented in Figure 3. The MIC & MBC values of ciprofloxacin ranging from 0.031 to 0.062 mg/mL and 0.062 to 0.0125 mg/mL against the tested organisms was taken as standard. The MIC & MBC values of the ligands and complexes ranged from 0.015 to 1.0 mg/mL against all the tested organisms. For *Escherichia coli* and *Klebsiella pneumoniae* the MIC and MBC value of complex 3 is lesser than that of ciprofloxacin, for complexes 4 and 7 the MIC and MBC value are comparable to ciprofloxacin.

4. Conclusions

In summary, we have successfully synthesized a series of mononuclear complexes of *p*-cymene ruthenium, benzene ruthenium, Cp* rhodium and Cp* Iridium containing thiosemicarbazide ligands. All these complexes were obtained in good yields and characterized by various spectroscopic studies like ¹H NMR, IR, UV-Vis and elemental analysis results obtained strongly supported the formation of the product. Spectroscopic data revealed that ligands coordinate to the metal centers through azomethine nitrogen and thiocarbonyl sulfur forming a five-membered chelate ring. Our effort to synthesize dinuclear complexes with L1 and L2 by using nitrogen in pyridine was unsuccessful. Furthermore, we have evaluated the antibacterial activity against the three different pathogenic bacteria *Staphylococcus aureus*, *Escherichia coli* and *Klebsiella pneumoniae*, standard antibiotic ciprofloxacin was taken as reference drug. Result attained clearly indicates that the formation of metal complexes enhanced the antibacterial activity compared to the free ligands. As proof from the inhibitory potency rhodium complexes shows good activity compare to Cp*Ir and *p*-cymene ruthenium complexes while benzene ruthenium complexes show minimum activity. Maximum complexes showed significant antibacterial activity for both Gram-positive and Gram-negative bacteria signifying their potential to be developed.

Supplementary Information (SI)

Figures S1-S27 and Tables S1-S2 are available at www.ias.ac.in/chemsci.

Acknowledgements

Agreeda Lapasam acknowledges the financial support of CSIR-HRDG, New Delhi in the form of SRF-NET award no. 09/347(0223)/2017-EMR-I. We thank Prof. A. K.

Singh, Department Biochemistry, NEHU Shillong for allowing us to use UV-Vis spectrophotometer. We thank Dr. Sanjay Adhikari and Smarling Suting for their help in Mass analysis and conductivity measurement. We thank NEHU-SAIF, Shillong, India for providing spectral studies.

References

- Caruso F, Pettinari R, Rossi M, Monti E, Gariboldi M B, Marchetti F, Pettinari C, Caruso A, Ramani M V and Subbaraju G V 2016 The in vitro antitumor activity of arene-ruthenium(II) curcuminoid complexes improves when decreasing curcumin polarity *J. Inorg. Biochem.* **162** 44
- Guerrero A, Oberhauser W, Riedel T, Peruzzini M, Dyson P J and Gonsalvi L 2017 New class of half-sandwich ruthenium(II) arene complexes bearing the water-soluble CAP ligand as an in vitro anticancer agent *Inorg. Chem.* **56** 5514
- Beckford F, Dourth D, Shaloski Jr M, Didion J, Thessing J, Woods J, Crowell V, Gerasimchuk N, Gonzalez-Sarrias A and Seeram N P 2011 Half-sandwich ruthenium-arene complexes with thiosemicarbazones: Synthesis and biological evaluation of [(η⁶-*p*-cymene) Ru(piperonalthiosemicarbazones)Cl]Cl complexes *J. Inorg. Biochem.* **105** 1019
- Caruso F, Pettinari R, Rossi M, Monti E, Gariboldi M B, Marchetti F, Pettinari C, Caruso A, Ramani M V and Subbaraju G V 2014 Synthesis, characterization, and antitumor activity of water-soluble (arene)ruthenium(II) derivatives of 1,3-Dimethyl-4-acylpyrazolon-5-ato ligands. First Example of Ru(arene)(ligand) antitumor species involving simultaneous Ru-N7(guanine) bonding and ligand intercalation to DNA *Inorg. Chem.* **53** 3668
- Keene F R, Smith J A and Collins J G 2009 Metal complexes as structure-selective binding agents for nucleic acids *Coord. Chem. Rev.* **253** 2021
- Chandra S, Tyagi M and Agrawal S 2010 Synthesis and characterization of a tetraaza macrocyclic ligand and its cobalt(II), nickel(II) and copper(II) complexes *J. Saudi Chem. Soc.* **75** 935
- Geldmacher Y, Oleszak M and Sheldrick W S 2012 Rhodium(III) and iridium(III) complexes as anticancer agents *Inorg. Chim. Acta* **393** 84
- Tang B, Wan D, Wang Y J, Yi Q Y, Guo B H and Liu Y J 2018 An iridium (III) complex as potent anticancer agent induces apoptosis and autophagy in B16 cells through inhibition of the AKT/mTOR pathway *Eur. J. Med. Chem.* **145** 302
- Yi Q Y, Wan D, Tang B, Wang Y J, Zhang W Y, Du F, He M and Liu Y J 2018 Synthesis, characterization and anticancer activity in vitro and in vivo evaluation of an iridium (III) polypyridyl complex *Eur. J. Med. Chem.* **145** 338
- Zhang W Y, Yi Q Y, Wang Y J, Du F, He M, Tang B, Wan D, Liu Y J and Huang H L 2018 Photoinduced anticancer activity studies of iridium(III) complexes targeting mitochondria and tubules *Eur. J. Med. Chem.* **151** 568

11. Simpson P V, Schmidt C, Ott I, Bruhn H and Schatzschneider U 2013 Synthesis, cellular uptake and biological activity against pathogenic microorganisms and cancer cells of rhodium and iridium N-Heterocyclic carbene complexes bearing charged substituent *Eur. J. Inorg. Chem.* **2013** 5547
12. Jain N, Alam P, Laskar I R and Panwar J 2015 Aggregation induced phosphorescence active iridium(III) complexes for integrated sensing and inhibition of bacterial growth in aqueous solution *RSC Adv.* **5** 61983
13. Demoro B, Sarniguet C, Sanchez-Delgado R S, Rossi M, Liebowitz D, Caruso F, Olea-Azar C, Moreno V, Medeiros A, Comini M A, Otero L and Gambino D 2012 New organoruthenium complexes with bioactive thiosemicarbazones as co-ligands: potential anti-trypanosomal agents *Dalton Trans.* **41** 1534
14. Adams M, Li Y, Khot H, De Kock C, Smith P J, Land K, Chibalea K and Smith G S 2013 The synthesis and antiparasitic activity of aryl- and ferrocenyl-derived thiosemicarbazone ruthenium(II)-arene complexes *Dalton Trans.* **42** 4677
15. Prabhakaran R, Kalaivani P, Huang R, Sieger M, Kaim W, Viswanathamurthi P, Dallemer F and Natarajan K 2011 Can geometry control the coordination behaviour of 2-hydroxy-1-naphthaldehyde-N(4)-phenylthiosemicarbazone? A study towards its origin *Inorg. Chim. Acta* **376** 317
16. Prabhakaran R, Renukadevi S V, Karvembu R, Huang R, Mautz J, Huttner G, Subashkumar R and Natarajan K 2008 Structural and biological studies of mononuclear palladium(II) complexes containing N-substituted thiosemicarbazones *Eur. J. Med. Chem.* **43** 268
17. Stacy A E, Palanimuthu D, Bernhardt P V, Kalinowski D S, Jansson P J and Richardson D R 2016 Zinc(II)-thiosemicarbazone complexes are localized to the lysosomal compartment where they transmetallate with copper ions to induce cytotoxicity *J. Med. Chem.* **59** 4965
18. Oliveira A A, Perdigo G M C, Rodrigues L E, da Silva J G, Souza-Fagundes E M, Jacqueline A, Takahashi W, Rocha R and Beraldo H 2017 Cytotoxic and antimicrobial effects of indium(III) complexes with 2-acetylpyridine-derived thiosemicarbazones *Dalton Trans.* **46** 918
19. King A P, Gellineau H A, Ahn J E, MacMillan S N and Wilson J J 2017 Bis(thiosemicarbazone) complexes of Cobalt(III). Synthesis, characterization, and anticancer potential *Inorg. Chem.* **56** 6609
20. Adams M, de Kock C, Smith P J, Land K M, Liu N, Hopper M, Hsiao A, Burgoyne A R, Stringer T, Meyer M, Wiesner L, Chibale K and Smith G S 2015 Improved antiparasitic activity by incorporation of organosilane entities into half-sandwich ruthenium(II) and rhodium(III) thiosemicarbazone complexes *Dalton Trans.* **44** 2456
21. Beckford F A, Leblanc G, Thessing J, Shaloski M Jr, Frost B J, Li L and Seeram N P 2009 Organometallic ruthenium complexes with thiosemicarbazone ligands: Synthesis, structure and cytotoxicity of $[(\eta^6\text{-p-cymene})\text{Ru}(\text{NS})\text{Cl}]^+$ (NS = 9-anthraldehyde thiosemicarbazones) *Inorg. Chem. Commun.* **12** 1094
22. Huang S, Zhu FW, Xiao Q, Zhou Q, Su W, Qiu H N, Hu B Q, Sheng J R and Huang C S 2014 Combined spectroscopy and cyclic voltammetry investigates the interaction between $[(\text{p-cymene})\text{Ru}(\text{benzaldehyde-N}(4)\text{-phenylthiosemicarbazone})\text{Cl}]\text{Cl}$ anticancer drug and human serum albumin *RSC Adv.* **4** 36286
23. Chellan P, Land K M, Shokar A, Au A, An S H, Clavel C M, Dyson P J, de Kock C, Smith P J, Chibale K and Smith G S 2012 Exploring the versatility of cycloplatinated thiosemicarbazones as antitumor and antiparasitic agents *Organometallics* **31** 5791
24. Arora S, Agarwal S and Singhal S 2014 Anticancer activities of thiosemicarbazides/ thiosemicarbazones: a review *Int. J. Pharm. Pharm. Sci.* **6** 34
25. Patel S R, Gangwal R, Sangamwar A T and Jain R 2014 Synthesis, biological evaluation and 3D-QSAR study of hydrazide, semicarbazide and thiosemicarbazide derivatives of 4-(adamantan-1-yl)quinoline as anti-tuberculosis agents *Eur. J. Med. Chem.* **6** 255
26. Tan O U, Ozadali K, Yogeewari P, Sriram D and Balkan A 2012 Synthesis and antimycobacterial activities of some new N-acylhydrazone and thiosemicarbazide derivatives of 6-methyl-4,5-dihydropyridazin-3(2H)-one *Med. Chem. Res.* **21** 2388
27. Umadevi P, Deepti K, Srinath I, Vijayalakshmi G and Tarakamji M 2012 Synthesis and in-vitro antibacterial activity of some new urea, thiourea and thiosemicarbazide derivatives *Int. J. Pharm. Pharm. Sci.* **4** 379
28. Mohareb R M and Mohamed A A 2012 Uses of 1-cyanoacetyl-4-phenyl-3-thiosemi carbazide in the synthesis of antimicrobial and antifungal heterocyclic compounds *Int. J. Pure Appl. Chem.* **2** 144
29. Rane R A, Naphade S S, Bangalore P K, Palkar M B, Shaikh M S, Karpoornath R 2014 Synthesis of novel 4-nitropyrrole-based semicarbazide and thiosemicarbazide hybrids with antimicrobial and anti-tubercular activity *Bioorg. Med. Chem. Lett.* **24** 3079
30. Zhang H J, Qian Y, Zhu D D, Yang X G and Zhu H L 2011 Synthesis, molecular modeling and biological evaluation of chalcone thiosemicarbazide derivatives as novel anticancer agents *Eur. J. Med. Chem.* **46** 4702
31. Adams M, Lia Y, Khota H, De Kock C, Smith P J, Land K, Chibale K and Smith G S 2013 The synthesis and antiparasitic activity of aryl and ferrocenyl derived thiosemicarbazone ruthenium(II)-arene complexes *Dalton Trans.* **42** 4677
32. Su W, Qian Q, Li P, Lei X, Xiao Q, Huang S, Huang C and Cui J 2013 Synthesis, characterization, and anticancer activity of a series of ketone-N⁴-substituted thiosemicarbazones and their Ruthenium(II) arene complexes *Inorg. Chem.* **52** 12440
33. Huang S, Peng S, Su W, Tang Z, Cui J, Huang C and Xiao Q 2016 In vitro interaction investigation between three Ru(II) arene complexes and human serum albumin: structural influences *RSC Adv.* **6** 47043
34. Fernández M, Arce E R, Sarniguet C, Morais T S, Tomaz A I, Azar C O, Figueroa R, Maya J D, Medeiros A, Comini M, Garcia M H, Otero L and Gambino D 2015 Novel ruthenium(II) cyclopentadienyl thiosemicarbazone compounds with antiproliferative activity on pathogenic trypanosomatid parasites *J. Inorg. Biochem.* **153** 306

35. Su W, Zhou Q, Huang Y, Huang Q, Huo L, Xiao Q, Huang S, Huang C, Chen R, Qian Q, Liu L and Li P 2013 Synthesis, crystal and electronic structure, anticancer activity of ruthenium(II) arene complexes with thiosemicarbazones *Appl. Organomet. Chem.* **27** 307
36. Yaman P K, Sen B, Karagoz C S and Subasi E J 2017 Half-sandwich ruthenium-arene complexes with thiophene containing thiosemicarbazones: Synthesis and structural characterization *Organomet. Chem.* **832** 27
37. (a) Lapasam A, Dkhar L, Joshi N, Poluri K M and Kollipara M R 2019 Antimicrobial selectivity of ruthenium, rhodium, and iridium half sandwich complexes containing phenyl hydrazone Schiff base ligands towards *B. thuringiensis* and *P. aeruginosa* bacteria *Inorg. Chim. Acta* **484** 255; (b) Lapasam A, Banothu V, Addepally U and Kollipara M R 2019 Synthesis, structural and antimicrobial studies of half-sandwich ruthenium, rhodium and iridium complexes containing nitrogen donor Schiff-base ligands *J. Mol. Struct.* **1191** 314
38. (a) Aradhyula B P R, Kalidasan M, Gangel K, Deb D K, Shepherd S L, Phillips R M, Poluri K M and Kollipara M R 2017 Synthesis, structural and biological studies of some half-Sandwich d^6 -metal complexes with pyrimidine-based ligands *Chem. Select.* **2** 2065; (b) Aradhyula B P R, Addepally U, Chiranjeevi T, Bethu M S, Yashwanth B, Rao J V, Poluri K M and Kollipara M R 2016 Synthesis, structural and in vitro functional characterization of arene ruthenium complexes with 1,3,5-tris(di-2-pyridylaminomethyl)benzene ligand *Inorg. Chim. Acta* **453** 284; (c) Sangilipandi S, Sutradhar D, Bhattacharjee K, Kaminsky W, Joshi S R, Chandra A K and Kollipara M R 2016 Synthesis, structure, antibacterial studies and DFT calculations of arene ruthenium, Cp^*_2Rh , Cp^*_2Ir and tricarbonylrhenium metal complexes containing 2-chloro-3-(3-(2-pyridyl)pyrazolyl)quinoxaline ligand *Inorg. Chim. Acta* **44** 95
39. Lapasam A, Hussain O, Phillips R M, Kaminsky W and Kollipara M R 2019 Synthesis, characterization and chemosensitivity studies of half-sandwich ruthenium, rhodium and iridium complexes containing $\kappa^1(S)$ and $\kappa^2(N,S)$ aroylthiourea ligands *J. Organomet. Chem.* **880** 272
40. Banothu V, Addepally U and Lingam J 2017 In vitro total phenolics, flavonoids contents, antioxidant and antimicrobial activities of various solvent extracts from the medicinal plant *PHYSALIS MINIMA LINN* *Int. J. Pharm. Pharm. Sci.* **9** 192
41. Banothu V, Addepally U, Suvarnalaxmi Ch, Chandrasekharnath N, Prakasham R S and Lingam J 2013 Antimicrobial property of *Datura* leaf extract against Methicillin-resistant *Staphylococcus aureus* isolated from Urethral and Skin Suppurative Infections *Curr. Trends Biotechnol. Pharm.* **7** 782
42. Banothu V, Neelagiri C, Addepally A, Lingam J and Bommareddy K 2017 Phytochemical screening and evaluation of *in vitro* antioxidant and antimicrobial activities of the indigenous medicinal plant *Albizia odoratissima* *Pharm. Biol.* **55** 1155
43. (a) Đilović I, Rubčić M, Vrdoljak V, Pavelić SK, Kralj M, Piantanida I and Cindrić M 2008 Novel thiosemicarbazone derivatives as potential antitumor agents: Synthesis, physicochemical and structural properties, DNA interactions and antiproliferative activity *Bioorg. Med. Chem.* **16** 5189; (b) Rogolino D, Bacchi A, De Luca L, Rispoli G, Sechi M, Stevaert A, Naesens L and Carcelli M 2015 Investigation of the salicylaldehyde thiosemicarbazone scaffold for inhibition of influenza virus PA endonuclease *J. Biol. Inorg. Chem.* **20** 1109
44. Anitha P, Manikandan R, Vijayan P, Anbuselvi S and Viswanathamurthi P 2015 Rhodium(I) complexes containing 9,10-phenanthrenequinone-N-substituted thiosemicarbazone ligands: Synthesis, structure, DFT study and catalytic diastereoselective nitroaldol reaction studies *J. Organomet Chem.* **79** 244
45. Kalaivani P, Prabhakaran R, Ramachandran E, Dallem F, Paramaguru G, Renganathan R, Poornima P, Vijaya Padmad V and Natarajan K 2012 Influence of terminal substitution on structural, DNA, Protein binding, anticancer and antibacterial activities of palladium(II) complexes containing 3-methoxy salicylaldehyde-4(N) substituted thiosemicarbazones *Dalton Trans.* **41** 2486
46. Ali I, Wani WA, Khan A, Haque A, Ahmad A, Saleem K and Manzoor N 2012 Synthesis and synergistic antifungal activities of a pyrazoline based ligand and its copper (II) and nickel(II) complexes with conventional antifungals *Microb. Pathog.* **53** 66